Supplementary Figures

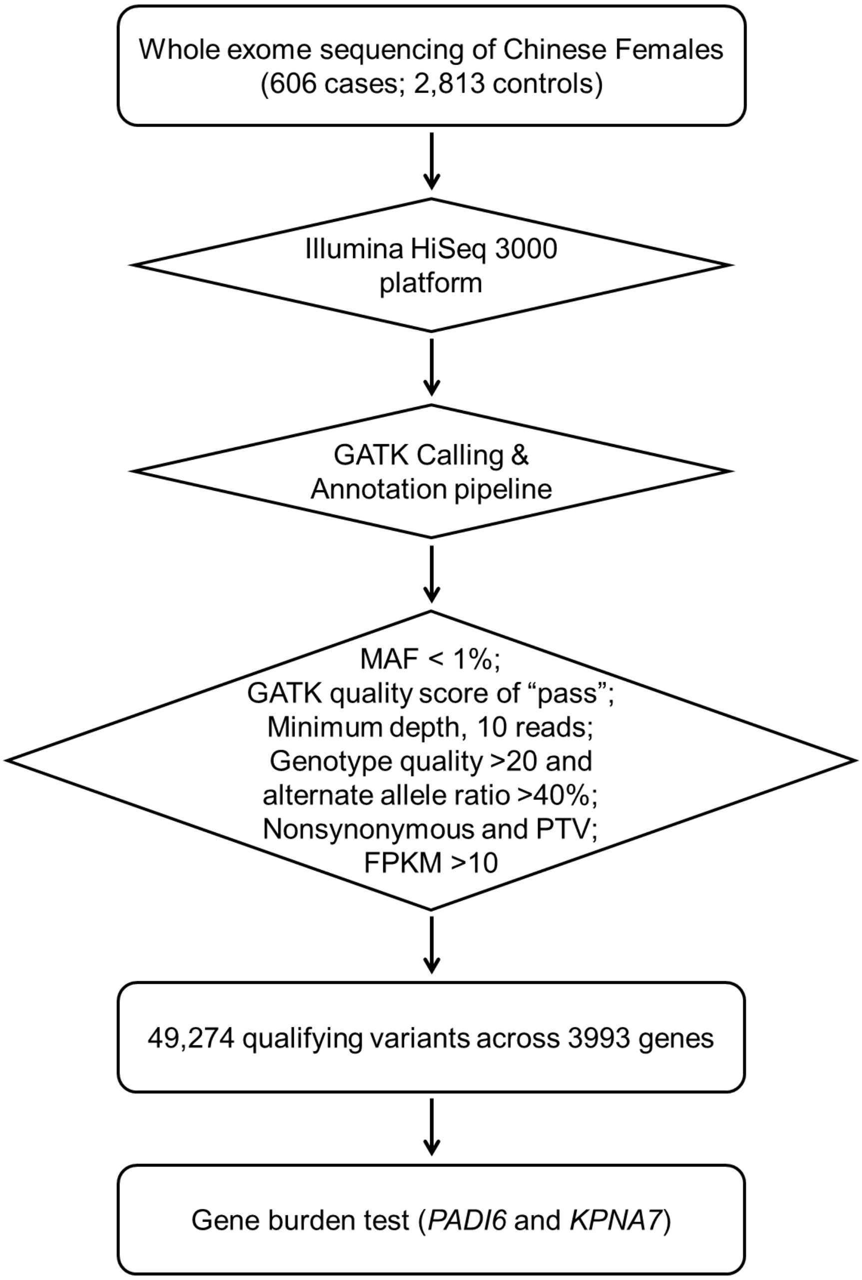

Supplemental Figure 1. Burden testing scheme

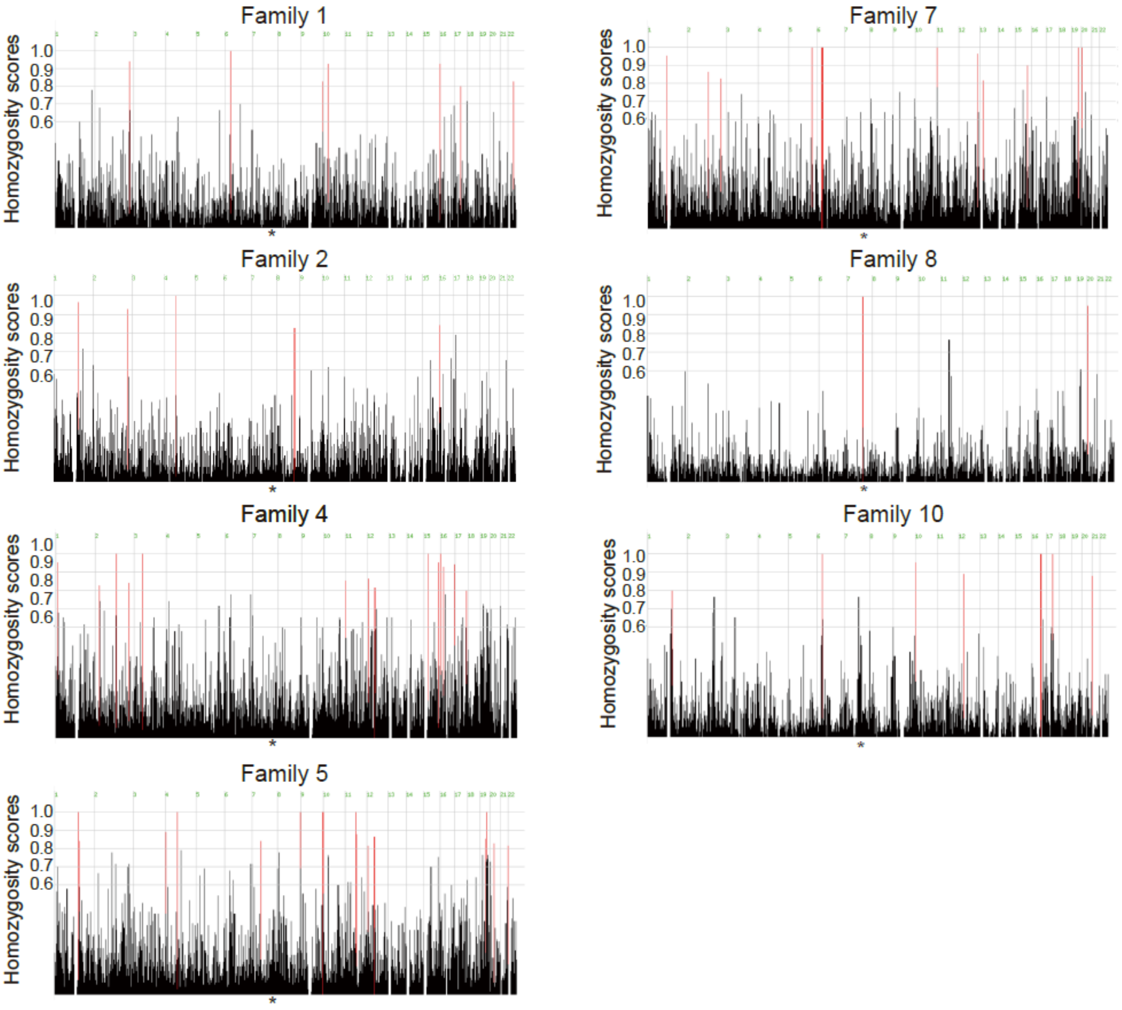

Supplemental Figure 2. Homozygosity mapping of patients carrying homozygous *KPNA7* variants

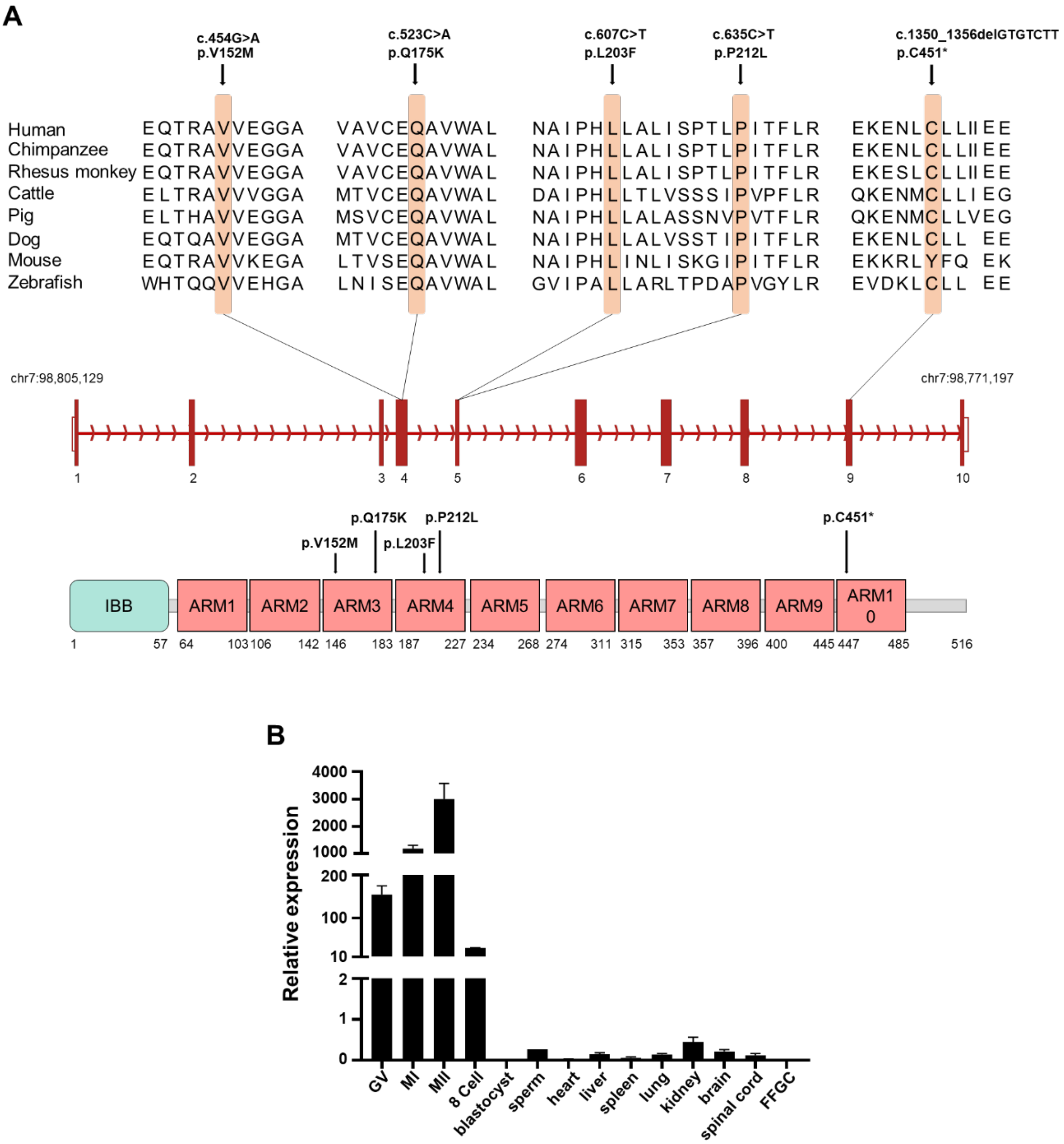

Supplemental Figure 3. Structure, conservation, and expression pattern of *KPNA7*

(**A**) The structure and protein domain architecture of KPNA7 and the location and conservation of the residues that were changed by the variants in *KPNA7*. IBB, importin β binding; ARM, armadillo. (**B**) The relative expression of *KPNA7* by Real-time qRT-PCT in developing human oocytes, early embryos, and several somatic tissues.

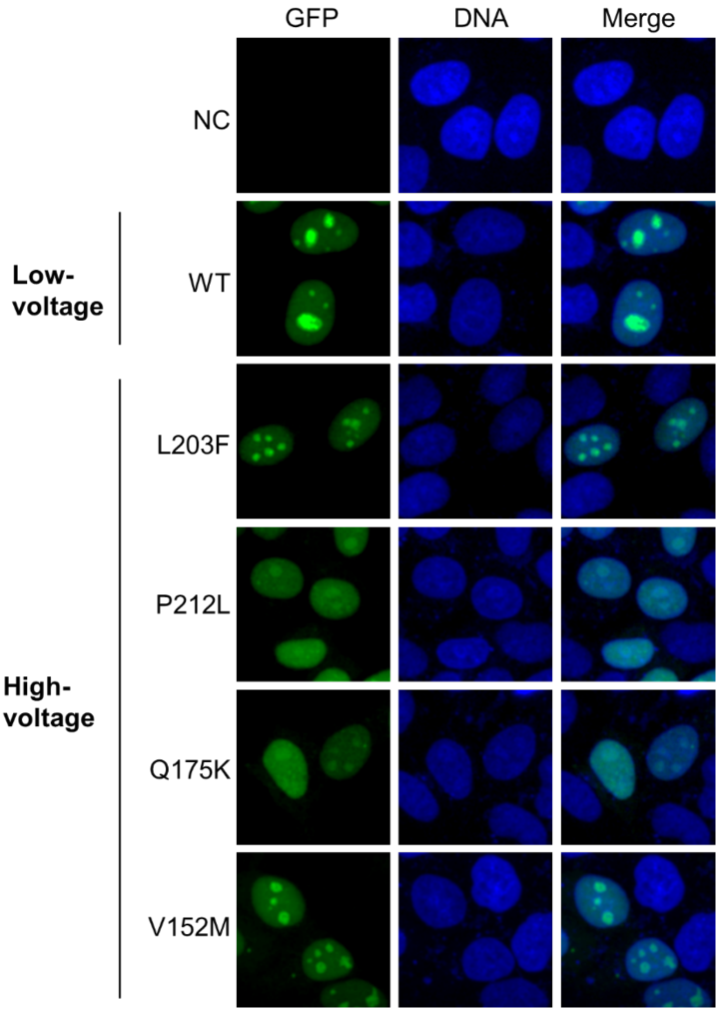

Supplemental Figure 4. Localization of GFP-tagged wild-type and mutant KPNA7 constructs in HeLa cells

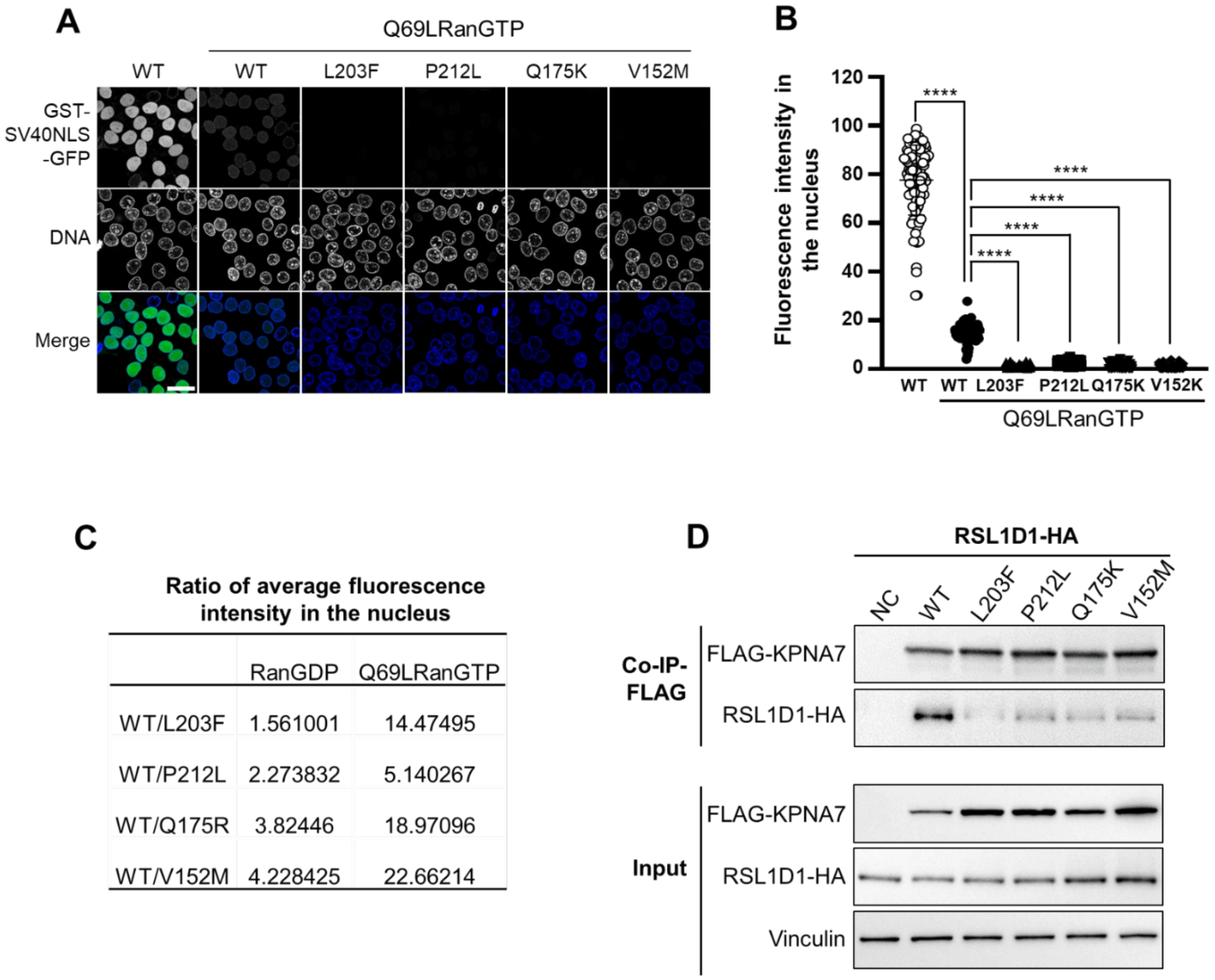

Ratio of average fluorescence intensity in the nucleus

	RanGDP	Q69LRanGTP
WT/L203F	1.561001	14.47495
WT/P212L	2.273832	5.140267
WT/Q175R	3.82446	18.97096
WT/V152M	4.228425	22.66214

Supplemental Figure 5. Effect of variants on the binding ability and transport capacity of KPNA7

(**A**) In vitro nuclear transport assays of purified wild-type and missense mutant KPNA7 with the transport substrate GST-SV40TNLS-GFP when added Q69RanGTP. GTP fixed Ran affected transport ability of KPNA7. DNA was stained with DAPI. Scale bar = 30 μm. (**B**) Quantitative analysis of KPNA7 transport capacity in (**A**). A total of 100 cells were counted. Data are shown as individual values with means ± s.d. One-way ANOVA. (**C**) Ratio of average fluorescence intensity in the nucleus by comparing wild-type group to mutant group. Functions of mutant KPNA7 were more sensitive to Q69LRanGTP. (**D**) Co-immunoprecipitation from HEK293T cells expressing FLAG-tagged wild-type or missense mutant KPNA7 and HA-tagged RSL1D1 with anti-FLAG beads. Missense alterations affect the interaction between KPNA7 and RSL1D1.

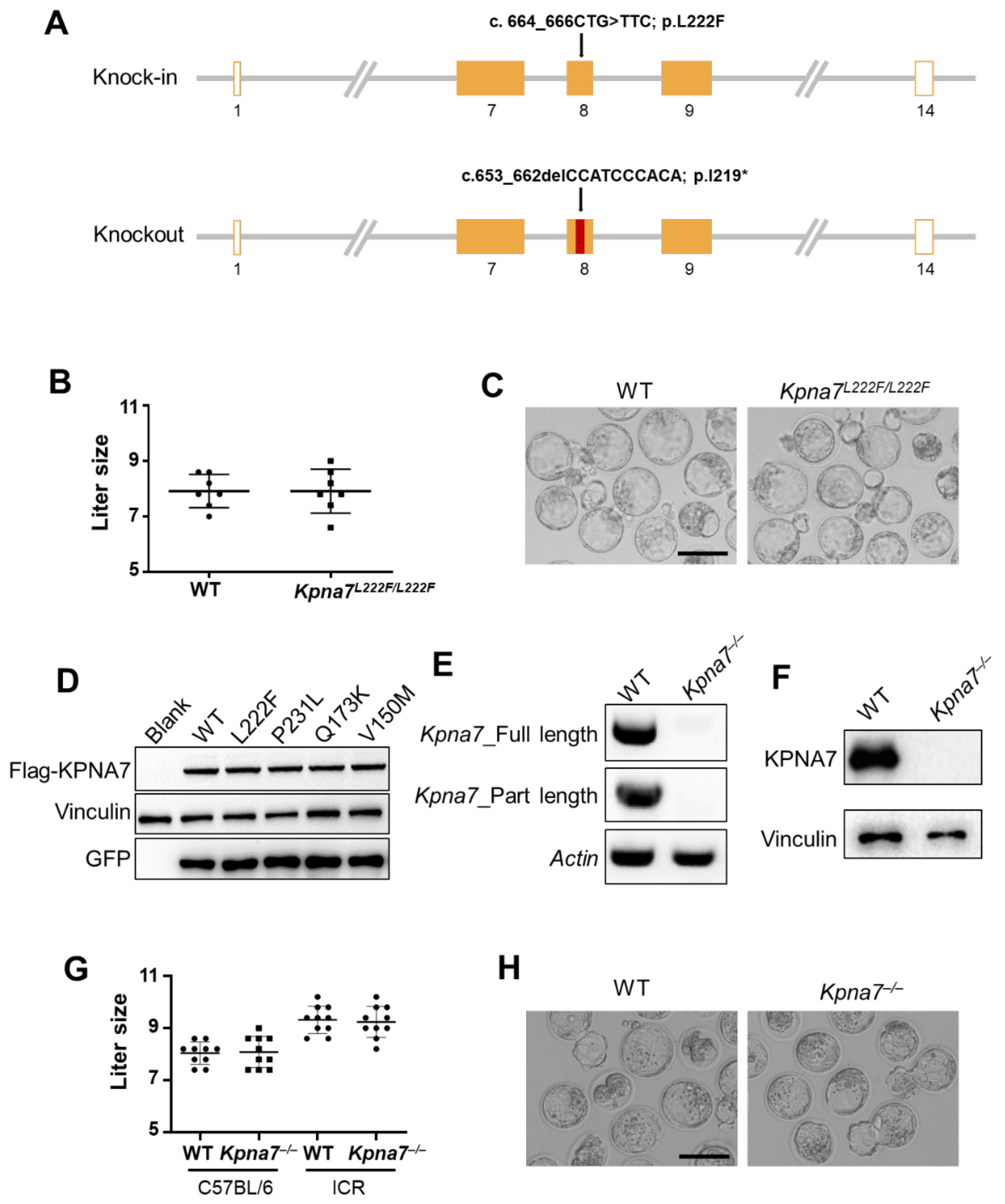

Supplemental Figure 6. Fertility of *Kpna7* knock-in and knockout female mice. (**A**) Schematic diagram of *Kpna7* L222F knock-in and knockout. The red box indicates the knockout area. (**B**) Statistical analysis of the reproductive ability of wild-type and *Kpna7*$^{\text{L222F/L222F}}$ mice in the C57BL/6 background. n = 7. Data are shown as individual values with means ± s.d. (**C**) In vitro embryonic development phenotype of wild-type and *Kpna7*$^{\mathrm{L222F/L222F}}$ mice. Scale bar = 100 μm. (**D**) Immunoblot of wild-type and missense mutant mouse KPNA7 proteins in HEK293T cells. Due to similar protein size of KPNA7 and GFP, blots were run in parallel. (**E**) RNA level of *Kpna7* in wild-type and *Kpna7*$^{-/-}$ oocytes. *Kpna7* was completely knocked out in *Kpna7*$^{-/-}$ oocytes. (**F**) Immunoblot of wild-type and *Kpna7*$^{-/-}$ oocytes. (**G**) Statistical analysis of the reproductive ability of *Kpna7*$^{-/-}$ mice in the C57BL/6 and ICR background. $n = 10$. Data are shown as individual values with means ± s.d. (**H**) In vitro embryonic development phenotype of wild-type and *Kpna7*$^{-/-}$ mice. Scale bar = 100 μm.

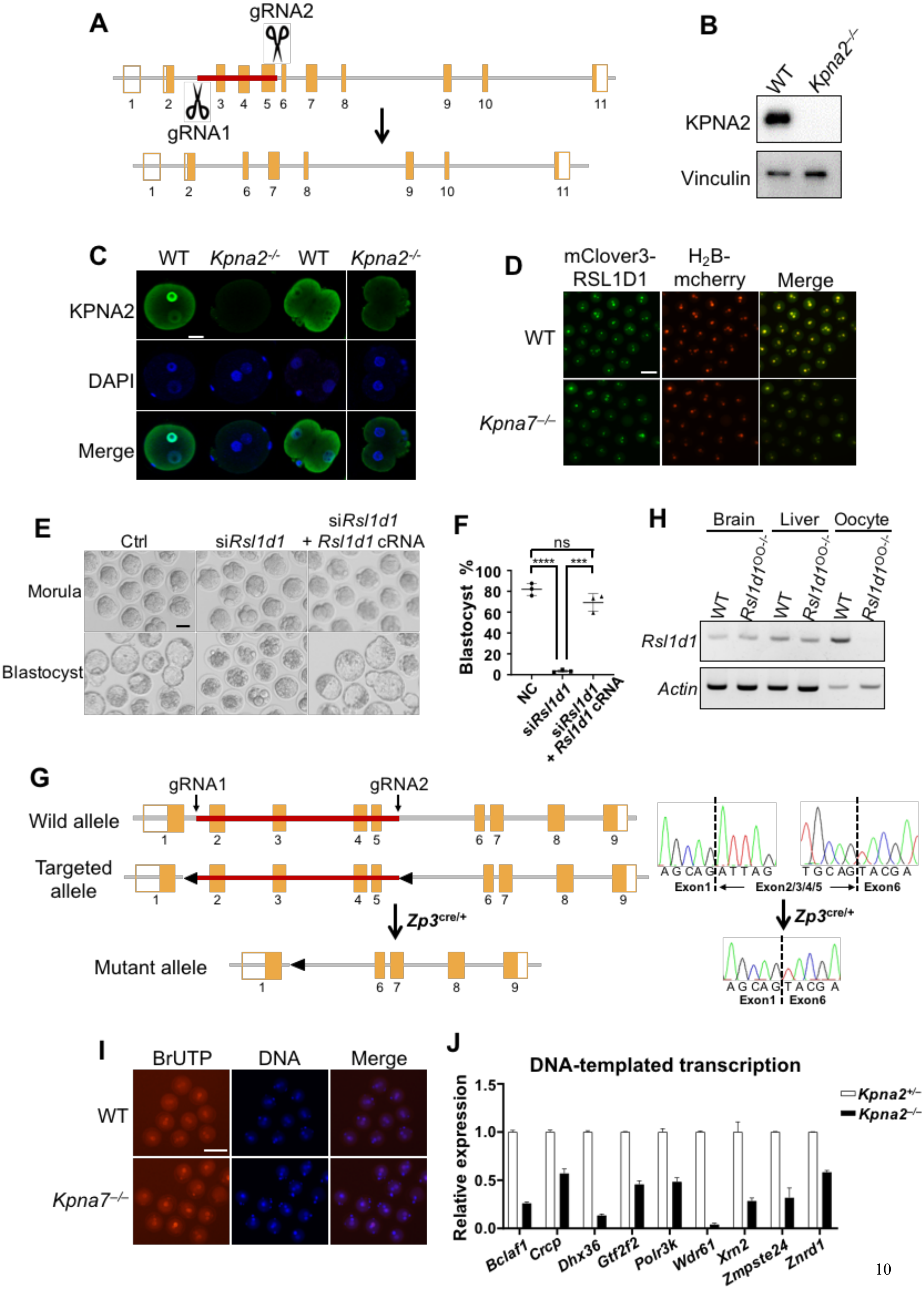
A
gRNA2
gRNA1
1 2 3 4 5 6 7 8 9 10 11
1 2 6 7 8 9 10 11
B
WT
Kpna2−/−
KPNA2
Vinculin
C
WT
Kpna2-/-
WT
Kpna2-/-
KPNA2
DAPI
Merge
D
mClover3-RSL1D1
H2B-mcherry
Merge
WT
Kpna7−/−
E
Ctrl
siRsl1d1
siRsl1d1 + Rsl1d1 cRNA
Morula
Blastocyst
F
ns
****
***
Blastocyst %
100
80
60
40
20
0
NC
siRsl1d1
siRsl1d1 + Rsl1d1 cRNA
H
Brain
Liver
Oocyte
WT
Rsl1d1OO-/-
WT
Rsl1d1OO-/-
WT
Rsl1d1OO-/-
Rsl1d1
Actin
G
gRNA1
gRNA2
Wild allele
1 2 3 4 5 6 7 8 9
Targeted allele
1 2 3 4 5 6 7 8 9
Zp3cre/+
Mutant allele
1 6 7 8 9
A G CA G A T T A G
T G C AG T A CG A
Exon1
Exon2/3/4/5
Exon6
Zp3cre/+
A G CA G T A CG A
Exon1
Exon6
I
BrUTP
DNA
Merge
WT
Kpna7−/−
J
DNA-templated transcription
Kpna2+/−
Kpna2−/−
Relative expression
1.5
1.0
0.5
0.0
Bclaf1
Crcp
Dhx36
Gtf2f2
Polr3k
Wdr61
Xrn2
Zmpste24
Znrd1

Supplemental Figure 7. Infertility of *Kpna2*$^{-/-}$ females and fertility of *Kpna7*$^{-/-}$ females.

(**A**) Schematic diagram of *Kpna2* knockout mice. The red box indicates the knockout area. (**B**) Immunoblot of wild-type and *Kpna2*$^{-/-}$ oocytes. (**C**) The expression and localization of endogenous KPNA2 in 1-cell and 2-cell embryos from wild-type and *Kpna2*$^{-/-}$ females fertilized with wild-type sperms in vitro. Scale bar = 20 μm. (**D**) Localization of RSL1D1 at 3 h after injection of mClover3-RSL1D1 cRNA into zygotes from wild-type and *Kpna7*$^{-/-}$ females. Scale bar = 100 μm. (**E**) In vitro embryonic development phenotype after *Rsl1d1* knockdown in mice and phenotypic rescue by mouse *Rsl1d1* cRNA injection into 2 PN zygotes. (**F**) Quantification of (**E**). Data are shown as individual values with means ± s.d. $n = 3$ biological replicates. Unpaired two-sided *t*-test. (**G**) Schematic diagram and Sanger sequencing confirmation of mice with an oocyte-specific knockout of *Rsl1d1*. The red box indicates the knockout area. (**H**) RNA level of *Rsl1d1* in oocytes and somatic tissues of wild-type and *Rsl1d1*$^{\text{OO-/-}}$ mice. *Rsl1d1* was completely knocked out in *Rsl1d1*$^{\text{OO-/-}}$ oocytes, while in somatic tissues, RNA level of *Rsl1d1* did not change. (**I**) Incorporation of BrUTP to mark the synthesis of nascent transcripts in zygotes from wild-type and *Kpna7*$^{-/-}$ females. Scale bar = 100 μm. (**J**) Real-time qRT-PCR analyses of down-regulated genes in 2-cell embryos from *Kpna2*$^{-/-}$ females compared to embryos from *Kpna2*$^{+/-}$ females. Data are shown as mean ± s.d.

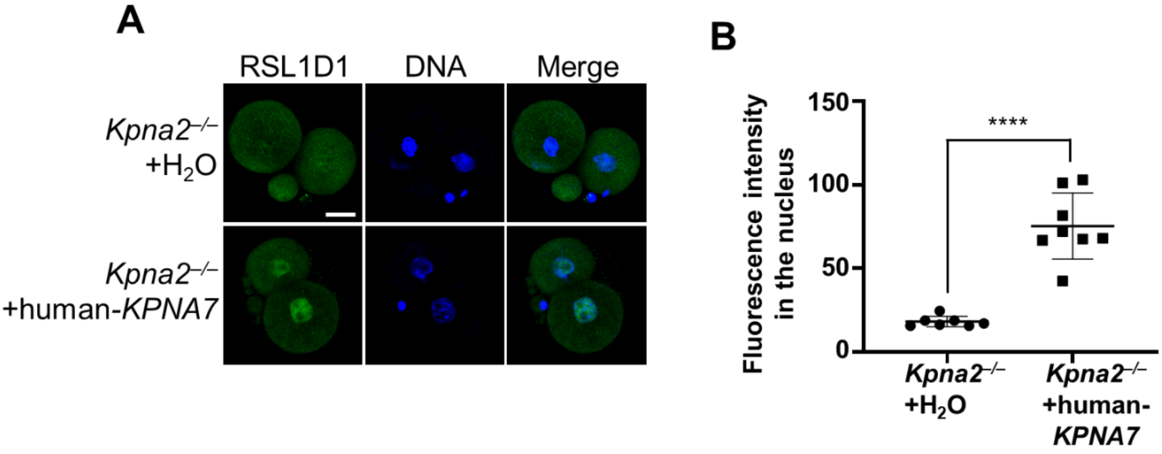

Supplemental Figure 8. Phenotypic rescue by cRNA injection.

(**A**) Molecular rescue by cRNA injection of human *KPNA7* into *Kpna2*$^{-/-}$ zygotes. After injection, the nuclear localization intensity of endogenous RSL1D1 in 2-cell embryos was stronger. (**B**) Fluorescence intensity of RSL1D1 in the nucleus of (**A**). Scale bar = 20 μm. Data are shown as individual values with means ± s.d. $n = 2$ biological replicates. Unpaired two-sided *t*-test.

Supplementary Tables

Supplemental Table 1. Overview of the *KPNA7* variants

Genomic Position on Chr 7 (bp)	cDNA Change	Protein Change	Variant Type	Inheritance[c]	Phenotype	ExAC[b]	GnomAD[b]	SIFT[a]	PPH2[a]
98,790,671	c.C607T	p.L203F	missense	AR	embryo arrest	1.41E-04	3.21E-04	D	P
98,790,643	c.C635T	p.P212L	missense	AR	embryo arrest	4.75E-05	6.02E-05	D	P
98,792,723	c.C523A	p.Q175K	missense	AR	embryo arrest	NA	NA	D	P
98,792,792	c.G454A	p.V152M	missense	AR	embryo arrest	NA	0.00003201	D	P
98,775,650	c.1350_1356delGTGTCTT	p.C451*	frameshift	AR	embryo arrest	NA	NA	NA	NA

[a] Variant assessment by SIFT and PolyPhen-2 (PPH2). D, damaging; P, probably damaging.

[b] Frequency of corresponding variants in ExAC Browser and gnomAD. NA, not available.

[c] AR, Autosomal recessive.

Supplemental Table 2. Clinical characteristics of the patients with *KPNA7* variants

Family	Age (years)	Duration of infertility (years)	IVF & ICSI cycles	Total oocytes retrieved	MII oocytes with normal morphology	Normal fertilized oocytes	Normal cleaved embryos	Usable embryos at day 3	Usable blastocysts	Outcome of embryo transfer
1	39	12	ICSI	20	20	18	18	0	0	/
			ICSI	10	8	6	6	0	0	/
			ICSI	2	2	2	2	0	0	/
			ICSI	37	28	19	18	2	0	Failure
			ICSI	28	16	16	14	2	0	/
2	31	3	IVF	19	17	16	12	2	0	/
			ICSI	22	20	14	13	5	0	/
3	37	7	IVF	5	2	2	2	0	/	/
			IVF	8	4	4	3	0	/	/
			IVF	10	8	8	8	2	0	Failure
			IVF	11	11	11	11	0	/	/
			IVF	1	1	1	1	0	/	/
			IVF	17	16	16	15	1	/	/
			ICSI	10	8	8	6	0	/	/
			ICSI	10	9	8	7	2	0	Failure
			ICSI	10	6	6	5	0	/	/
			ICSI	15	10	10	9	2	/	/
			ICSI	22	15	15	11	4	0	Failure

4	39	8	ICSI	8	unknown	0	/	/	/	/
			ICSI	12	6	4	4	0	/	/
5	34	8	IVF	10	8	8	unknown	4	0	/
			IVF	9	6	6	unknown	0	/	/
			IVF	11	8	unknown	unknown	0	/	/
6	44	15	ICSI	13	unknown	4	4	0	/	/
			ICSI	4	unknown	2	2	2	/	Failure
			ICSI	8	unknown	6	unknown	0	/	/
7	35	8	ICSI	18	17	7	7	0	2	Failure
			ICSI	9	6	6	5	2	/	Embryo arrest at 12 weeks
			ICSI	6	6	6	5	2	/	Failure
			ICSI	12	7	7	7	1	0	Failure
8	29	3	IVF	5	5	3	3	0	/	/
			ICSI	10	10	8	8	2	/	Failure
9	28	5	IVF	20	20	14	14	2	0	/
10	36	7	IVF	7	unknown	unknown	unknown	0	0	/
			ICSI	2	2	2	2	0	0	/

/ refers to not applicable

Supplemental Table 3. Results of NCBI/Blastp

Description	Sequence ID
Transcription initiation factor TFIID subunit 1	XP_047298347.1
Transcription initiation factor TFIID subunit 1-like	NP_722516.1
KIAA2022	EAW98638.1
TAF4 RNA polymerase II	NP_003176.2
TBP-associated factor 1 isoform 2 variant	BAD92553.1
FACT complex subunit SPT16	NP_009123.1
Human TFIID bound to promoter DNA and TFIIA	6MZM_D
TBP-associated factor	AAC50901.1
Dystonia 3 (with Parkinsonism)	CAM98556.1
RSL1D1 protein	AAI07783.1
SURF6 protein	AAH03001.1
Unnamed protein product	BAG51440.1
Structure of the histone chaperone CIA/ASF1-double bromodomain complex linking histone modifications and site-specific histone eviction	3AAD_A
Myosin phosphatase Rho-interacting protein	XP_011522064.1
Rho-interacting protein 3	BAC78198.1
MPRIP protein	AAH09982.2
N-acetyltransferase ESCO1	NP_443143.2
Establishment of cohesion 1 homolog 1	AAH89426.1
Intermediate filament family orphan 2	NP_001129737.1
Probable RNA-binding protein 19	NP_001140170.1
Unnamed protein product	BAB14757.1

Splicing factor YJU2	NP_060544.2
Crystal Structure of Ubl123 with an EZH2 peptide	6P5L_D
Biorientation of chromosomes in cell division protein 1-like 1 isoform X1	XP_011512129.1
Zinc finger protein 40	NP_002105.3
Human immunodeficiency virus type I enhancer binding protein 1	EAW55310.1

Supplemental Table 4. In vitro development of *Kpna2*$^{-/-}$ embryos (n = 6)

		Incubation			
		24 h	48 h	72 h	108 h
WT	Fragmented/degenerated	0	0	5	23
	One-cell	2	2	1	1
	Two-cell	149	12	9	6
	Four-cell		137	0	0
	Morula			136	2
	Blastocyst				119
Kpna2$^{-/-}$	Fragmented/degenerated	8	3	15	82
	One-cell	19	10	9	5
	Two-cell	128	142	102	62
	Four-cell	1	1	30	7
	Morula			0	0
	Blastocyst				0

Supplemental Table 5. In vitro development of *Rsl1d1*$^{\text{OO-/-}}$ embryos (n = 4)

		Incubation			
		24 h	48 h	72 h	108 h
WT	Fragmented/degenerated	0	0	0	14
	One-cell	0	0	0	0
	Two-cell	72	4	0	0
	Four-cell		68	4	0
	Morula			68	0
	Blastocyst				58
Rsl1d1$^{\text{OO-/-}}$	Fragmented/degenerated	2	9	19	23
	One-cell	20	15	8	7
	Two-cell	40	37	33	30
	Four-cell		1	2	2
	Morula			0	0
	Blastocyst				0

Supplemental Table 6. Primers used for plasmid construction and real-time PCR

Primer name	Sequence (5’-3’)	Application
PCMV6-Flag-KPNA7-F	GAGGCGATCGCATGGATTACAAGGATGACGACGATAAGCCGACCTTAGATGCTCCAGAA	PCR for plasmid construction
PCMV6-Flag-KPNA7-R	GCGACGCGTCTATTTTTTGCTAAGCATTCATAATCTATAAATTCATAATCTTGGTCT	
PCMV6-Flag-mKpna7-F	GAGGCGATCGCATGGATTACAAGGATGACGACGATAAGGCTACCTCAAAGGCTCCCAAA	
PCMV6-Flag-mKpna7-R	GCGACGCGTTCACACTCTCAGCCCAGGCCCGGGC	
hKPNA7-203-F	TTCCTAGCCTTGATTTCACCCACCCTGCCG	
hKPNA7-203-R	ATGTGGGATGGCATTGCTTGTGATGACGTT	
hKPNA7-212-F	TGATCACATTTCTGCGGAACATCACGTGGA	
hKPNA7-212-R	GCAGGGTGGGTGAAATCAAGGCTAGGAGAT	
hKPNA7-175F	AAGGCAGTGTGGGCTCTTGGTAA	
hKPNA7-175-R	TTCACACACAGCCACGTTGGAGG	
hKPNA7-152-F	ATGGTAGAAGGGGGAGCCATCC	
hKPNA7-152-R	GGCACGAGTCTGCTCCGAAG	
hKPNA7-451-F	CTGATAGAAGAACTTGGTGGGATCGAT	
hKPNA7-451-R	AGGTTTTCCTTCTCAGACCGTTTCT	
mKpna7-222-F	TTCATCAACCTTATTTCAAAAGGCATACCAATC	
mKpna7-222-R	GTGTGGGATGGCATTATTGGAGATGAC	
mKpna7-231-F	TAATCACATTTCTTCGGAACATCTCATGGAC	
mKpna7-231-R	GTATGCCTTTTGAAATAAGGTTGATCAGGTGTGG	

mKpna7-173-F	AAGGCAGTGTGGGCCCTTGGGAATA	
mKpna7-173-R	CTCAGACACTGTCAGGTGTGGGGAA	
mKpna7-150-F	ATGGTGAAAGAGGGTGCCATTCAG	
mKpna7-150-R	AGCTCGGGTCTGCTCTGAAG	
PCMV6-hKPNA2-Ha-F	GAGGCGATCGCATGTCCACCAACGAGAATGCTAAT	
PCMV6-hKPNA2-Ha-R	GCGACGCGTAAAGTTAAAGGTCCCAGGAGCCCCAT	
PCMV6-mKpna2-Ha-F	GAGGCGATCGCATGTCCACGAACGAGAATGCTAACTTACC	
PCMV6-mKpna2-Ha-R	GCGACGCGTGAAGTTAAAGGTCCCAGGAGCTCCAT	
pGEX4T-mRSL1D1-GFP-F	CGCGTGGATCCCCGGAATTCATGGAGGATTCGGCCTCGGC	
RSL1D1-GFP-R	AGTTCTTCTCCTTTACTGGTCGACTGGGGTACTTTGGG	
RSL1D1-GFP-F	CCCCAGTCGACCAGTAAAGGAGAAGAACTTTTCACTGGAGTTG	
pGEX4T-mRSL1D1-GFP-R	GTCAGTCACGATGCGGCCGCCTATTTGTATAGTTCATCCATGCCATGTGTAATCCC	
PCMV6-hRSL1D1-Ha-F	AGATCTGCCGCCGCGATCGCATGGAGGATTCGGCCTCGG	
PCMV6-hRSL1D1-Ha-R	TCGAGCGGCCGCGTACGCGTGGTCGACTGGGGTACTTTGGG	
PCMV6-mRSL1D1-Ha-F	GATCTGCCGCCGCGATCGCATGAAGGGCTCTGCGTCCG	
PCMV6-mRSL1D1-Ha-R	TCGAGCGGCCGCGTACGCGTGTTTGAGTGGGCCGCCTTG	
mRSL1D1-sysnmut-F	GTCTGCTTATTCACAAAAGATGAATTCGATTCACC	
mRSL1D1-sysnmut-R	GTCGGATGATTCGGAGAGAATGCTATGAGGCAAAG	
pCR3.1-mClover-mRSL1D1-F	CTTCAGATCTGGTTACGCGTATGAAGGGCTCTGCGTCCGAATC	
pCR3.1-mClover-mRSD1-R	TTCTGGATATACCACAGCGATCGCCTAGTTTGAGTGGGCCGCCTTG	
KPNA7-mRT-F	GACATCATTTCTTATCTCCTCCAG	For real-time quantitative PCRs
KPNA7-mRT-R	GCAAACTGTCACCATCTCCATC	
KPNA6-mRT-F	CACTGCTGGCAACAGGGCTCAA	

KPNA6-mRT-R	GCAGCCCAGTGATACCAGGTAC
KPNA4-mRT-F	CAATCTCATAGAAGAATGTGGTG
KPNA4-mRT-R	CTCTGTTGGTACATTGGTCGAT
KPNA3-mRT-F	TGAGATCATAGAAGAGTGTGGAG
KPNA3-mRT-R	TGAAGGTTGGCTGTTGGGTC
KPNA2-mRT-F	TGATGCTACTTCTCCGCTACAG
KPNA2-mRT-R	GGATGATGTTGTCTATAGGAGG
KPNA1-mRT-F	ACAGCTGGAAATAGGGCACAGA
KPNA1-mRT-R	GATACAACCCAGTTCTACTAGGTAC
KPNA7-hRT-F	GTGATGGCCCAGAGTTCAGAGATAA
KPNA7-hRT-R	CATCCGAGAGAACCTCACTGTCCTG
KPNA6-hRT-F	GCATTCAGCTCCGGAAGCAGAA
KPNA6-hRT-R	GTGTGGTTGCTAACTGCAGGT
KPNA5-hRT-F	TAGTTCCACTGTACCCATTCCAGAG
KPNA5-hRT-R	TCTCTGTACAACTCCTGGTTTCTGT
KPNA4-hRT-F	ACTATGAGAAGACAACGAAATGAAGTTG
KPNA4-hRT-R	TAGCAGCTTGAACTGCACTTAATTG
KPNA3-hRT-F	TGAAGTGACAGTGGAACTGCGGAAG
KPNA3-hRT-R	CTTGCTGCCTGGACAGCACTCAATT
KPNA2-hRT-F	GAAATGAGGCGTCGCAGAATAGAGG
KPNA2-hRT-R	CTGGCAGCTTGAGTAGCTTGGAG
KPNA1-hRT-F	CAGATTAGTAACATGGAGATGGCACCA
KPNA1-hRT-R	CCACAAACCTGGCCACTACTCCT
GAPDH-hRT-F	GGAGCGAGATCCCTCCAAAAT

GAPDH-hRT-R	GGCTGTTGTCATACTTCTCATGG
ACTB-hRT-F	ATGATGATATCGCCGCGCTC
ACTB-hRT-R	AATCCTTCTGACCCATGCCC
Kpna2-mRT-F	TGATGCTACTTCTCCGCTACAG
Kpna2-mRT-R	GGATGATGTTGTCTATAGGAGG
Kpna7-mRT-F	GACATCATTTCTTATCTCCTCCAG
Kpna7-mRT-R	GCAAACTGTCACCATCTCCATC
Actb-mRT-F	CAGCTTCTTTGCAGCTCCTT
Actb-mRT-R	AGTCCTTCTGACCCATTCCCA
Bclaf1-mRT-F	ATGGCACCTGTTCCTCTTGACG
Bclaf1-mRT-R	GAGGCAGCTTAATGTGGTCAAAG
Crcp-mRT-F	CAAAGAGCAGCGGAAGGAGAGT
Crcp-mRT-R	GACAATCGCTGGACTCTGGTTC
Polr3k-mRT-F	AGAAGTGGACGACGTGCTTGGT
Polr3k-mRT-R	AGAAGGTGGTCATTGGCTCGTC
Znrd1-mRT-F	GTCTGTGGATGAGGGACCTGAA
Znrd1-mRT-R	AGACCGTCTGTCCTTCATCAGC
Zmpste24-mRT-F	CTACTCAGAGGTGGAAGGCACT
Zmpste24-mRT-R	ACAGCAGGAACACCAATGACTGA
Xrn2-mRT-F	CAGTTTGGACACGAGGTCAAGG
Xrn2-mRT-R	ACTCTCGAAGGACATTCAGCCG
Gtf2f2-mRT-F	ACAGTGTTTACGGAGAGCTCCTCAG
Gtf2f2-mRT-R	CAGCTGTTGTGAGAGCCTTACAGGT
Wdr61-mRT-F	GCTCCTTGTCACGGCTTCAGAT

Wdr61-mRT-R	GTGTCATCAGGACAGAACGCAAC
Dhx36-mRT-F	GTCTTTCTACCAGGCTGGGACA
Dhx36-mRT-R	GTGTCTGGTTGACGGTAGGCAT
Aars-mRT-F	CCAATCAGACTCCAGTGGTAGC
Aars-mRT-R	GCTCCGCATAGAAACAGGTCTTGT

Abbreviations: F forward, R reverse